JOURNAL OF AGRICULTURAL AND FOOD CHEMISTRY

pubs.acs.org/JAFC Article

Rational Development of a New Reaction-Based Ratiometric Fluorescent Probe with a Large Stokes Shift for Selective Detection of Bisulfite in Tap Water, Real Food Samples, Onion Tissues, and Zebrafish

Gangqiang Yuan, Liyi Zhou,* Qiaomei Yang, Haiyuan Ding, Libin Tan, and Longpeng Peng

Cite This: J. Agric. Food Chem. 2021, 69, 4894−4902 Read Online

ACCESS | Metrics & More | Article Recommendations | Supporting Information

ABSTRACT: Bisulfite (HSO_3^-) is usually widely added to tap water and food because it has antibacterial, bleaching, and antioxidant effects. However, its abnormal addition would cause a series of serious diseases related to it. Therefore, development of an effective method for HSO_3^- detection was of great significance to human health. In this work, a new reaction-based ratiometric fluorescent probe KQ−SO_2 was rationally designed, which could be used for the highly selective detection of $HSO3^-$ in tap water, real food samples, onion tissues, and zebrafish. Specifically, a positively charged benzo[*e*]indolium moiety and a carbazole group through a condensation reaction resulted in KQ−SO_2, which displayed two well-resolved emission bands separated by 225 nm, fast response (1 min), and high selectivity and sensitivity toward $HSO3^-$ upon undergoing the Michael addition reaction, as well as low cytotoxicity in vitro. In addition, KQ−SO_2 has been successfully applied for the detection of HSO_3^- in tap water, real food samples, onion tissues, and zebrafish with satisfactory results. We predict that KQ−SO_2 could be used as a powerful tool to reveal the relationship between $HSO3^-$ and the human health.

KEYWORDS: *bisulfite, fluorescent probe, fluorescence imaging, Michael addition reaction, real food samples*

INTRODUCTION

Bisulfite ($HSO3^-$) as a food additive had a long history of development in food processing due to its antibacterial, bleaching, and antioxidant effects.[1,2] However, a large amount of intake led to disturbances in the body's circulatory system.[3] In the past few decades, studies showed that excessive uses of $HSO3^-$ could cause respiratory tract mucosal thickening, nasopharyngitis, neurological disorders, heart and lung diseases, and other diseases.[4−7] In order to avoid excessive sulfur residues in foods causing adverse reactions such as edible poisoning, many countries formulated a series of standards to strictly control the intake of sulfur. For instance, food with more than 20 mg/L sulfites should be marked as per the U.S. Food and Drug Administration (FDA) guidelines.[8,9] The maximum usage of sulfur dioxide in wine should not exceed 0.25 mg/kg in China.[10] Motivated by these needs, we urgently need to develop some novel, reliable, rapid, and convenient methods for $HSO3^-$ detection in real samples and biological systems.

In recent years, the fluorescence detection imaging technology has shown many advantages, such as real-time detection, simple operation, less damage to the object under test, high sensitivity, and high selectivity, and has attracted more and more attention from scientific researchers.[11−15] Until now, many fluorescent sensors for detecting SO_2 were developed, which is based on nucleophilic addition reactions with the electron-deficit "C═C", ketone, or aldehyde groups and inhibition of C═N isomerization. However, there are also many challenges for rapid and highly selective detection in real samples and biological systems. For instance, low selectivity due to the influence of some nucleophiles in food samples; the response linear range of the probe could not satisfy the low concentration of $SO3^{2-}$/$HSO3^-$ in food samples; certain foods had high background signals, difficult preparation processes, and autofluorescence interference; the reliability, precision, and reproducibility need to be improved, when these probes were used to detect the concentration of $SO3^{2-}$/$HSO3^-$ in food samples. Therefore, in the process of designing responsive small-molecule probes, we should consider and solve these problems, which could improve the practicability of the probes in food samples.[16] This is because in water, real food samples, and biological systems, SO_2 mainly existed in the forms of $HSO3^-$. Compared with organic solvents, water as a solvent reduced the sensitivity of fluorescent sensors.[17] In order to solve this problem, related studies reported that the cyanine dye had good water solubility, large maximum absorption wavelengths and fluorescence quantum yields, and so forth because the α,β-unsaturated bonds (Michael addition reaction) were easily added by nucleophiles to form the $-SO_3H$ adducts and could be used to detect $HSO3^-$.[18,19] In addition, most of the previously reported $HSO3^-$ sensors were disturbed

Received: January 28, 2021
Revised: March 14, 2021
Accepted: April 2, 2021
Published: April 14, 2021

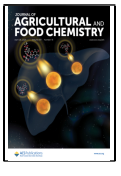

by the single-channel signal output or interfered by light crosstalk between channels during imaging due to the small Stokes shift. Moreover, they were susceptible to interference from various factors, such as instruments, environments, and the concentration of sensor molecules. Compared with ratiometric sensors, which had a built-in correction of the dual-emission peak, could eliminate most of these interferences, or if not all. Therefore, development of some new ratiometric fluorescent sensors with a large Stokes shift for $HSO3^-$ detection will be highly desired to reduce the crosstalk of light between channels and increase the precision of the sensors.

In this work, we designed a cationic ratiometric sensor (KQ−SO_2) for hemicyanine dye derivatives, which was obtained by the condensation reaction of carbazole formaldehyde with positively charged indoline. The sensor KQ−SO_2 had a maximum emission of 600 nm with an orange fluorescence emission. After the addition of $HSO3^-$, KQ−SO_2 could provide a α,β-unsaturated C═C bond binding site for the Michael addition reaction with $HSO3^-$.[20−22] Through the Michael addition reaction, the ICT process was blocked and emitted blue fluorescence to achieve ratiometric $HSO3^-$ detection. The unique response site and the large Stokes shift (225 nm) met the need for $HSO3^-$ detection *in vitro* with a rapid response time and high selectivity and sensitivity. In addition, the newly designed cationic ratiometric sensor (KQ−SO_2) was not only successfully utilized to detect $HSO3^-$ in food but also was applied to a biological model of zebrafish.

MATERIALS AND METHODS

Chemicals and Instruments. Unless otherwise noted, all chemicals were obtained from commercial suppliers, and no further purification was required for use. 9-Ethylcarbazole, 2,3,3-trimethylindolenine, piperidine, and dimethyl sulfoxide-d_6 (DMSO-d_6) were all purchased from Adamas Reagent Co., Ltd. (Shanghai, China). All reactions were carried out on magnetic stirrers, and their reaction process was monitored by thin layer chromatography (TLC). TLC was performed using silica gel 60 F_{254}, and column chromatography was performed on silica gel (200−300 mesh), both of which were obtained from Qingdao Ocean Chemical Company (Qingdao, China). The fluorescence intensity was measured at 5.0 nm and 5.0 nm excitation and emission slits on the G-9800A fluorescence spectrometer, respectively. Real food samples were purchased from a local supermarket (Changsha, China).

Synthesis and Characterization of the Probe KQ−SO_2. *Synthesis of N-Ethyl-3-carbazolecarboxaldehyde.* 1 mL of DMF and 0.15 g (1 mmol) of $POCl_3$ were prepared in a 50 mL round-bottomed flask equipped with a stirring bar; then, 0.8 g of **1** (4 mmol) and 10 mL of CH_3Cl were added into the flask. The reaction mixture was refluxed for 12 h. After that, the reaction was stopped and cooled to room temperature.[23] The solvent was removed by rotary evaporation, and the crude product was removed without further purification to directly use in the following synthesis.

*Synthesis of 1,2,3,3-Tetramethyl-3H-indolium Iodide (**4**).* In a 25 mL round-bottomed flask equipped with a magnetic stirrer, 0.2 g (1.25 mmol) of 2,3,3-trimethylindolenine was dissolved in 5 mL of toluene, and then, 0.2 g (1.43 mmol) of methyl iodide was added, and the reaction mixture was heated at 100 °C for 20 h under N_2 protection.[24] After the reaction, the reaction mixture was cooled to room temperature, and then, the solid was vacuum filtered and dried in a vacuum drying oven, without further purification in the next synthesis.

Synthesis of the Fluorescent Sensor KQ−SO_2. 0.4 g of **2** (1.8 mmol) and 0.3 g of **4** (1 mmol) were added to a 100 mL round-bottomed flask containing 20 mL of absolute ethanol and 0.5 mL of piperidine; the reaction mixture was stirred at 80 °C for 4 h under N_2 protection, and then, the mixture was subjected to rotary evaporation and purified by column chromatography (DCM/MeOH/HAc = 100:1:1, v/v/v) to afford KQ−SO_2 as a purple solid with a yield of 80%.[1] H NMR (400 MHz, DMSO-d_6): 9.14 (s, 1H), 8.68−8.64 (d, J = 16.0 Hz, 1H), 8.41−8.39 (d, J = 8.0 Hz, 1H), 8.28−8.26 (d, J = 8.0 Hz, 1H), 7.89−7.85 (dd, J_1 = 8.0 Hz, J_2 = 4.0 Hz, 3H), 7.74−7.61 (t, J = 26.0 Hz, 2H), 7.61−7.57 (m, 3H), 7.40−7.36 (t, J = 8.0 Hz, 1H), 4.59−4.54 (dd, J_1 = 8.0 Hz, J_2 = 4.0 Hz, 2H), 4.17 (s, 3H), 1.65 (s, 6H), 1.40−1.36 (t, J = 8.0 Hz, 3H); ^{13}C NMR (100 MHz, DMSO-d_6): δ(ppm) 181.57, 155.59, 143.67, 143.41, 142.42, 140.85, 129.44, 129.34, 129.10, 127.48, 126.26, 125.39, 123.28, 122.83, 121.22, 121.04, 115.03, 110.75, 110.70, 109.76, 56.49, 52.15, 34.53, 26.27, 19.04, 14.35; LC−MS: m/z $[C_{27}H_{27}N_2]^+$, calcd 379.22; found, 378.74.

Spectrophotometric Measurements. Fluorescence measurement experiments were measured in 10 mM phosphate buffer solution with DMSO as cosolvent solution (H_2O/DMSO = 99:1, v/v). The pH value of PBS solution used was from 4.0 to 10.0, which was achieved by adding minimal volumes of HCl solution or NaOH solution. Fluorescence emission spectra were recorded at an excitation wavelength of 375 nm with an emission wavelength range from 385 to 740 nm. A 1 mM stock solution of probe KQ−SO_2 was prepared by dissolving KQ−SO_2 in DMSO. The procedure of calibration measurements with KQ−SO_2 in the buffer with different SO_2 concentration is as follows: 5 μL of stock solution of KQ−SO_2 and 1993 μL of PBS buffer solution with 2 μL of different $NaHSO_3$ concentration solutions were combined to afford a test solution, which contained 5.0 μM of KQ−SO_2 to obtain the test sample. The solutions of various testing species were prepared from F^- (NaF), Cl^- (NaCl), Br^- (KBr), I^- (KI), $N3^-$ (NaN_3), $NO2^-$ ($NaNO_2$), $NO3^-$ ($NaNO_3$), AcO^- (NaAcO), $PO4^{3-}$ (K_3PO_4), $HPO4^{2-}$ (K_2HPO_4), SCN^-(NaSCN), HS^- (NaHS), ClO^- (NaClO), Cys, GSH, and Hcy, using twice-distilled water with final concentrations of 100 μM.

Detection of $HSO3^-$ in Real Food Samples. Zebrafish (Guangzhou China), Lycium chinensis (the Ningxia Hui Autonomous Region China), deionized water (20 mL), and tap water (20 mL) were from a local area (Changsha china). Prior to the HSO_3^- analysis, the fish samples and Lycium chinensis samples were respectively treated with deionized water, sonicated for 3 min, and filtered with an organic membrane to prepare water samples. A 20 μL solution of each sample was used to determine the HSO_3^- content in the solution. The above experiment was repeated three times for each sample, and the fluorescent signal of the sample was recorded at I_{475}/I_{600}.

Cell Cytotoxic Assays and Onion Tissue and Zebrafish Imaging. MTT analysis was used to evaluate the cytotoxicity of HeLa cells. The sensor was added to the incubated cells, and the microplate reader was used for spectrophotometric determination at 575 nm. The percentage of viability of control cells and probe-treated cells represented the toxicity of the probe, and the above experiment was repeated three times for each sample. Next, for imaging $HSO3^-$ in onion tissues, the onion tissues were incubated with 5.0 μM KQ−SO_2 for 30 min at 37 °C and washed three times with PBS, and then, 20.0 μM $HSO3^-$ was added for 30 min. Before imaging, onion tissues were washed with PBS three times. Fluorescence images were acquired with an Olympus FV 1000-MPE.

BiospaceLab PhotonIMAGER Imaging for Zebrafish. 5.0 μM KQ−SO_2 and 20.0 μM $HSO3^-$ were injected into the abdominal position by hypodermic injection in the same area; zebrafish were incubated with KQ−SO_2 at 37 °C for real-time imaging. The fluorescence emission was collected at the blue channel (460−490 nm) and red channel (580−650 nm) when excited at 450 nm.

Statistical Analysis. All data are expressed as means ± s.e.m. The data are accumulated under each condition from at least three independent experiments. The statistical analyses are performed using the Student's t-test.

Other Methods. Additional experimental information and results (chemistry and biology) are provided in the Supporting Information

https://doi.org/10.1021/acs.jafc.1c00592
J. Agric. Food Chem. 2021, 69, 4894−4902

Scheme 1. Synthetic Route for the Reaction-Based Fluorescent Probe KQ−SO_2; (a) DMF, $POCl_3$, $CHCl_2$, Reflux, 12 h; (b) Toluene, under N_2, 100 °C, 20 h; (c) Absolute Ethanol, Piperidine, N_2, 80 °C, 4 h

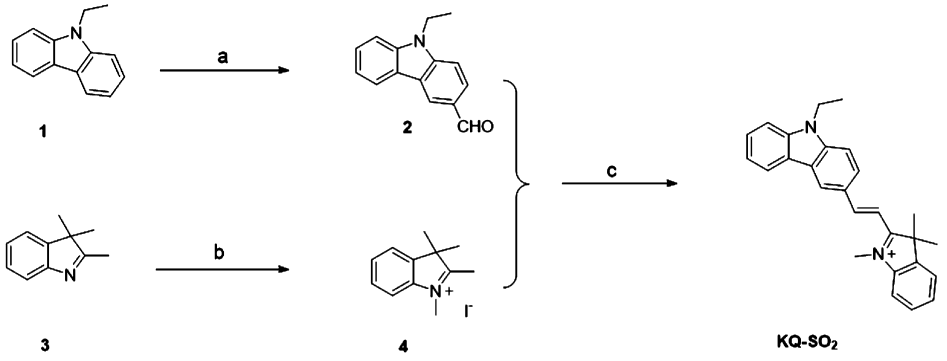

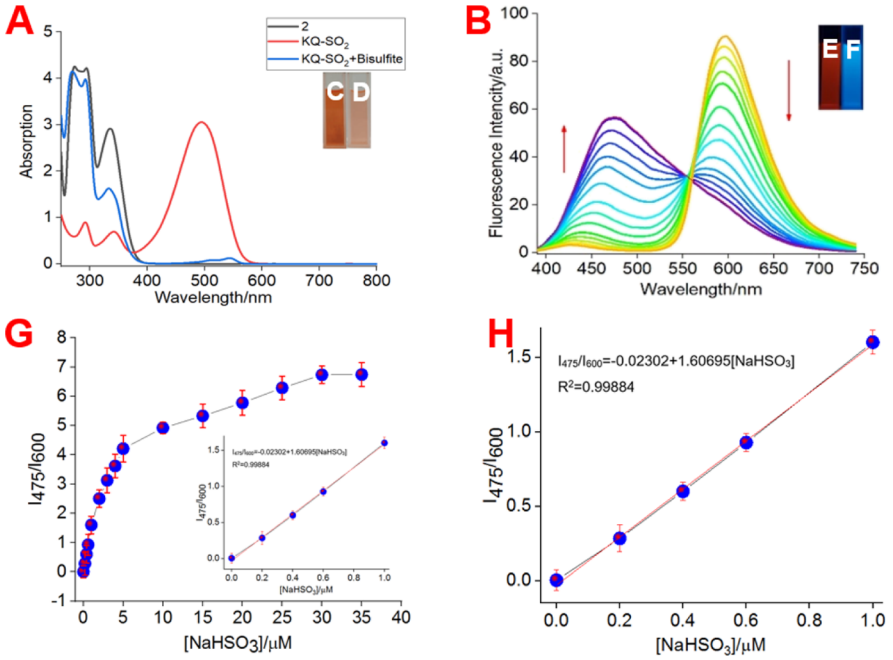

Figure 1. (A) UV/vis absorption spectra of 5.0 μM KQ−SO_2, 5.0 μM **2**, and 5.0 μM KQ−SO_2 response to 20 μM $HSO3^-$ in 10 mM PBS buffer (pH 7.4); (C, D) naked-eye confirmation of color change of KQ−SO_2 under visible light; the photographs of KQ−SO_2 in the absence (left) or presence (right) of 40 μM $HSO3^-$; (B) fluorescence spectra of 5.0 μM KQ−SO_2 in the presence of concentrations of $HSO3^-$ (0−40.0 μM) in 10 mM PBS buffer (pH 7.4), excited at 375 nm; (E, F) photographs of KQ−SO_2 solution in the absence (left) or presence (right) of 40 μM $HSO3^-$ under 365 nm UV radiation; (G) calibration curve of fluorescence ratio (I_{475}/I_{600}) *vs* $HSO3^-$ concentration (0−40.0 μM) ; (H) plot of fluorescence ratio (I_{475}/I_{600}) *vs* the concentration of $HSO3^-$ (0−1.0 μM).

RESULTS AND DISCUSSION

Design and Synthesis of the Probe KQ−SO_2. In order to obtain a better detection and imaging resolution, a ratiometric sensor KQ−SO_2 was synthesized in this work in three steps, as shown in Scheme 1. This sensor was composed of *N*-ethyl-3-carbazolecarboxaldehyde and 1,2,3,3-tetramethyl-3*H*-indolium iodide conjugated together in a yield of 80%. We introduced the indoline group to endow the sensor with good hydrophilicity due to its well-known hydrophilic group. This design not only solved the problem of hydrophilicity but also provided specific reaction sites of $HSO3^-$ for the Michael addition reaction and realized the ratiometric detection of $HSO3^-$ in real-food samples and biological models. The structure of KQ−SO_2 was fully characterized by ^{1}H NMR, ^{13}C NMR, and ESI−MSS analyses (see the Supporting Information).

Spectral Response to Bisulfite. We discuss the *in vitro* sensing performance of sensor KQ−SO_2 for $HSO3^-$ in the 10 mM PBS buffer solution (1% DMSO, pH 7.4). Figure 1A shows the UV/vis absorption of 5.0 μM KQ−SO_2 or **2** and 5.0 μM KQ−SO_2 incubated with 40 μM $HSO3^-$. The sensor has a broad absorption band (320−580 nm); among them, KQ−SO_2 had a remarkable absorption at 500 nm; upon addition of $HSO3^-$, it would decrease rapidly and match well with the carbazole derivatives between 320 to 350 nm. We further tested the sensor's fluorescence response to $HSO3^-$; the results are shown in Figure 1B. In the absence of $HSO3^-$, the sensor exhibited only an emission band at 600 nm, while in the presence of $HSO3^-$ (0−40 μM), the reaction was blue-shifted due to the Michael addition reaction of $HSO3^-$ with KQ−SO_2. Moreover, KQ−SO_2 had a large Stokes shift 225 nm and a considerable distance of 225 nm between the two emission peaks of 475 and 600 nm. Figure 1B indicated that the disappearance of a long-wavelength band at 600 nm and the

https://doi.org/10.1021/acs.jafc.1c00592
J. Agric. Food Chem. 2021, 69, 4894−4902

Table 1. Comparison of Detection Methods for HSO_3^- Derivatives

Methods	LOD	Examination range	Detection time	Real food inspection	Structure	Reference
UV–vis	4μg /L	–	–			1
HPLC	21μg /L	10-250mg/L	-	√		2
spectrophotometric	5.6 mg/L	10-250mg/L	70s	√		3
Capillary electrophoretic	0.1mM	0.01-0.5mM	-			4
HPLC	1.5 mg/L	-	8min	√		5
spectrophotometric	10 ng/mL	0.03-25 μ g/mL	-	√		6
capillary electrophoretic	2 μ M	10-800 μ M	-	√		7
enzyme electrode	10ppm	-	3-5min			8
electrochemical sensor	100 ppb	0.1 – 2 ppm	2.5min			9
CdSe nanoparticles	36 μg/L	–	>30 min			10
Flow-injection fluorimetric	85 nM		30s		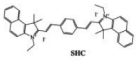	11
Two-Photon Fluorescent Probe	0.09 μ M		Within sec		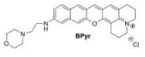	12
Ratiometric Fluorescent Probe	5.6×10^{-9} M		<90s	√	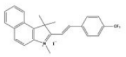	13
Reversible Fluorescent Probe	7.3×10^{-7}M		<5s		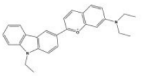	14
two-photon-based fluorescent probe	0.39 μM		<5s		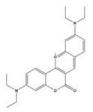	15
Ratiometric fluorescent probe	2.67nM	–	<90s		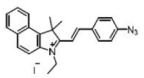	16
Molecular Rotor-Based fluorescent probe	7.9×10^{-5} M	–			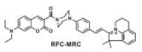	17
ICT-based fluorescent probe	13.1 nM		30min		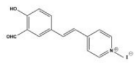	18
water-soluble fluorescent probe	8.3nM		<15s		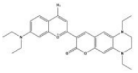	19
Ratiometric fluorescent probe	0.29 μM		<2min	√	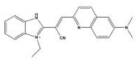	20
Reaction-Based Ratiometric fluorescent probe	10.28 nM		<1min	√	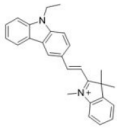	This work

https://doi.org/10.1021/acs.jafc.1c00592
J. Agric. Food Chem. 2021, 69, 4894−4902

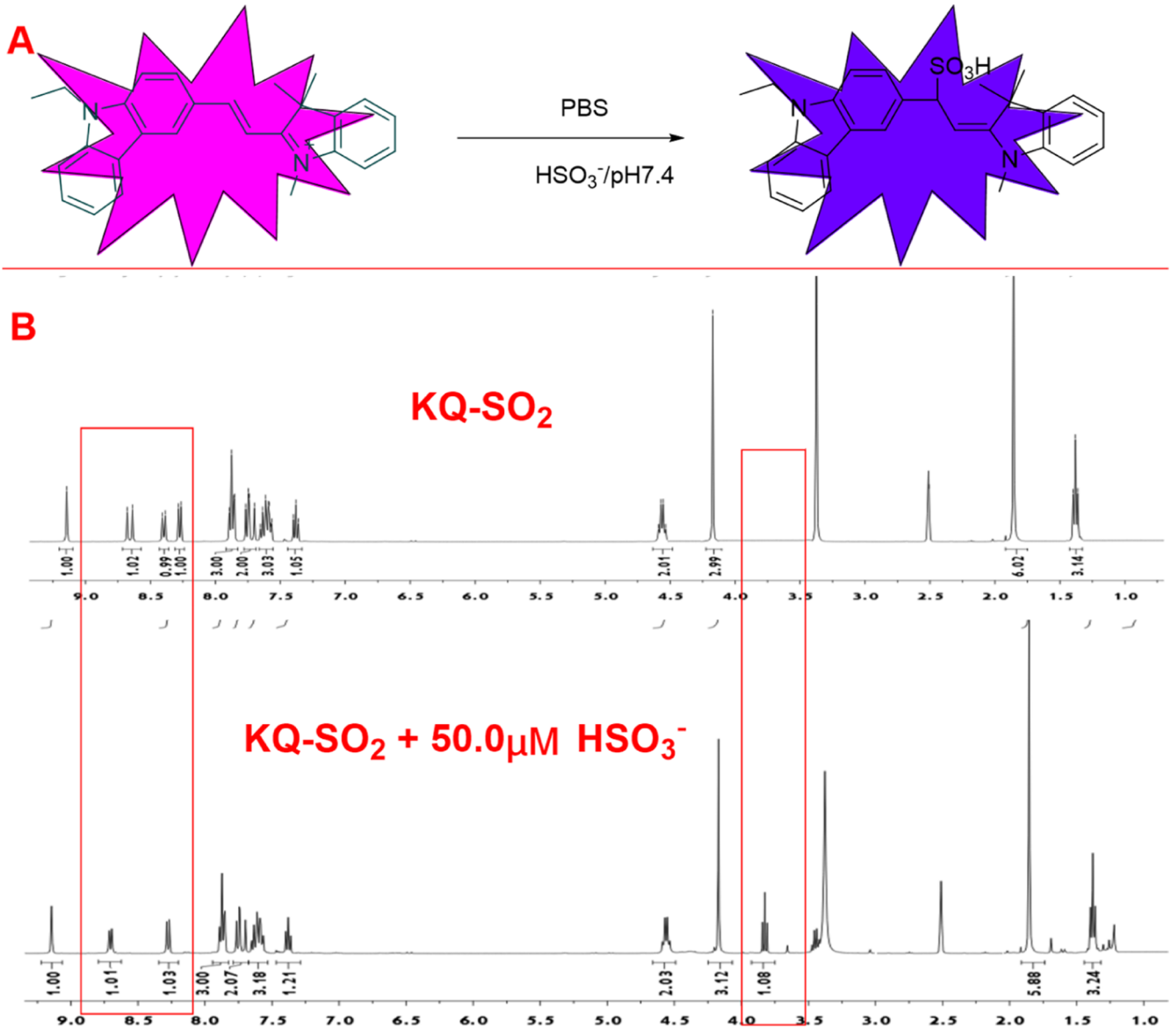

Figure 2. Proposed sensing mechanism of KQ−SO_2 response to HSO3$^-$. (A) KQ−SO_2 undergoes a Michael addition reaction with HSO3$^-$; (B) ^{1}H NMR characterization of KQ−SO_2 before (DMSO-d_6) and after (DMSO-d_6 + D_2O + 20 μM HSO3$^-$) response to HSO3$^-$.

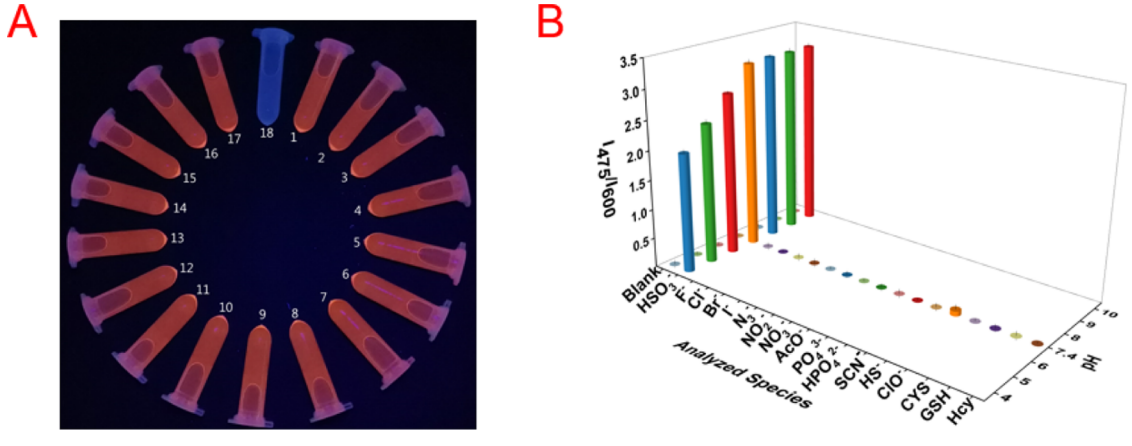

Figure 3. (A) Photograph of KQ−SO_2 (5.0 μM) upon addition of various species in 10 mM PBS buffer (pH 7.4, 1% DMSO) under 365 nm UV radiation. (1, blank; 2, F^-; 3, Cl^-; 4, Br^-; 5, I^-; 6, N3$^-$; 7, NO2$^-$; 8, NO3$^-$; 9, AcO^-; 10, $PO4^{3-}$; 11, $HPO4^{2-}$; 12, SCN^-; 13, HS^-; 14, ClO^-; 15, Cys; 16, GSH; 17, Hcy; 18, HSO3$^-$). The acquisition of photograph 5 min after mixing; (B) Fluorescence ratio ($F_{475nm}/F_{600\ nm}$) of KQ−SO_2 with various species and pH (4.0−10.0) when excited at 375 nm.

https://doi.org/10.1021/acs.jafc.1c00592
J. Agric. Food Chem. 2021, 69, 4894−4902

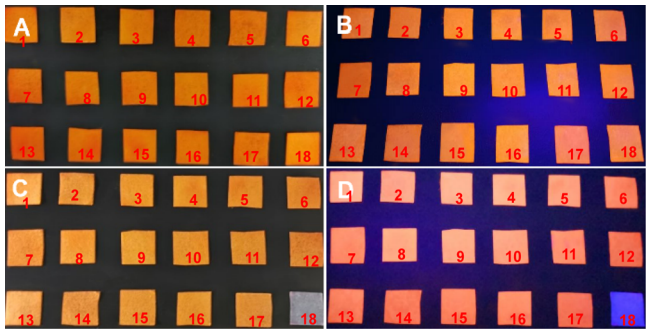

Figure 4. Photograph of the neutral filter papers subjected to various species (1, blank; 2, F^-; 3, Cl^-; 4, Br^-; 5, I^-; 6, $N3^-$; 7, $NO2^-$; 8, $NO3^-$; 9, AcO^-; 10, $PO4^{3-}$; 11, $HPO4^{2-}$; 12, SCN^-; 13, HS^-; 14, ClO^-; 15, Cys; 16, GSH; 17, Hcy; 18, $HSO3^-$) under visible light and 365 nm UV radiation.

appearance of a short-wavelength band at 475 nm due to the ICT process were destroyed by the $HSO3^-$ addition reaction with sensor KQ–SO_2 of the α,β-unsaturated bond to induce π-conjugation system blocking, thereby achieving $HSO3^-$ ratiometric detecting. Moreover, as expected, when excited at 375 nm, as the $HSO3^-$ concentration changed from 0 to 40.0 μM, fluorescence emission of KQ–SO_2 at 475 nm increased significantly and at 600 nm, decreased rapidly and was accompanied by the color changes from red to blue (Figure 1E,F). Therefore, the probe KQ–SO_2 displayed a good colorimetric and ratiometric fluorescence response to $HSO3^-$. The ratiometric response (I_{475}/I_{600}) of KQ–SO_2 was linear with the change of $HSO3^-$ concentration (0–1.0 μM). The detection limit of the KQ–SO_2 response to $HSO3^-$ was calculated as low as 10.28 nM (Figure 1G,H). Thus, this implies that the sensor may quantitatively detect $HSO3^-$ within a certain minimal concentration range. More impressively, the response of the sensor KQ–SO_2 to $HSO3^-$ exhibited more excellent analytical performance compared to other reported detection methods for $HSO3^-$ derivatives; the results are shown in Table 1.

In order to study the mechanism of KQ–SO_2 response to $HSO3^-$, we performed mass spectrometry analysis and ^{1}H NMR. It was clearly observed that the signal of m/z (378.76) corresponds to KQ–SO_2 (Figure S1). In addition, a mass peak

Table 2. Determination of the Concentration of Bisulfite in Real Food Samples

sample	$HSO3^-$ level (μmol/L)	added (μmol/L)	found (μmol/L)	recovery (%)
fish	0.0231	0.1000	0.1240	100.7
		0.3000	0.3239	100.2
Lycium chinensis	0.0324	0.1000	0.1322	99.85
		0.3000	0.3316	99.76
deionized water	0.0000	0.1000	0.1010	101.0
		0.3000	0.3003	100.3
tap water	0.0177	0.1000	0.1163	98.81
		0.3000	0.3170	99.78

at m/z (482.18) corresponds to KQ–SO_2 + $HSO3^-$ (Figure S1). Moreover, the ^{1}H NMR results also clearly show the displacement of H atoms before and after reacting KQ–SO_2 with $HSO3^-$ with remarkable changes, as shown in Figure 2. Thus, the mechanism of the probe for sensing $HSO3^-$ was most likely based on the Michael addition reaction of double C=C bonds.

Selectivity and pH Effects. The effect of selectivity and pH on the fluorescence intensity ratio (I_{475}/I_{600}) of KQ–SO_2 was then carried out. First, as shown in Figure 3A,B, we investigated the reaction of KQ–SO_2 (5.0 μM) with various potential interfering species (100 μM); the results showed that the exception of $HSO3^-$, blank, F^-, Cl^-, Br^-, I^-, $N3^-$, $NO2^-$, $NO3^-$, AcO^-, PO_4^{3-}, HPO_4^{2-}, SCN^-, HS^-, ClO^-, Cys, GSH, and Hcy could not show remarkable fluorescence changes at 600 and 475 nm upon excitation at 375 nm. This was to say; the sensor had an excellent selectivity for $HSO3^-$ over other species. In addition, we measured the fluorescence efficiency of $HSO3^-$ for the sensor under different pH (4.0–10.0) conditions. As demonstrated in Figure 3B, the sensor showed that the fluorescence intensity ratio (I_{475}/I_{600}) was more effective under neutral and alkaline conditions than under acidic conditions, indicating that the reaction between $HSO3^-$

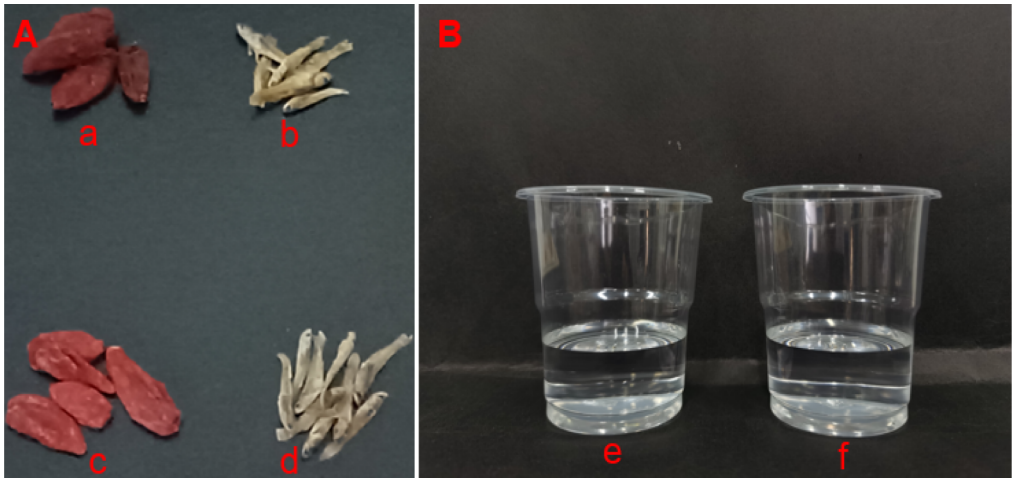

Figure 5. (A) Photograph of real food samples: (a, b) normal food samples and (c, d) polluted food samples; (B) photograph of deionized water (e) and tap water (f).

https://doi.org/10.1021/acs.jafc.1c00592
J. Agric. Food Chem. 2021, 69, 4894–4902

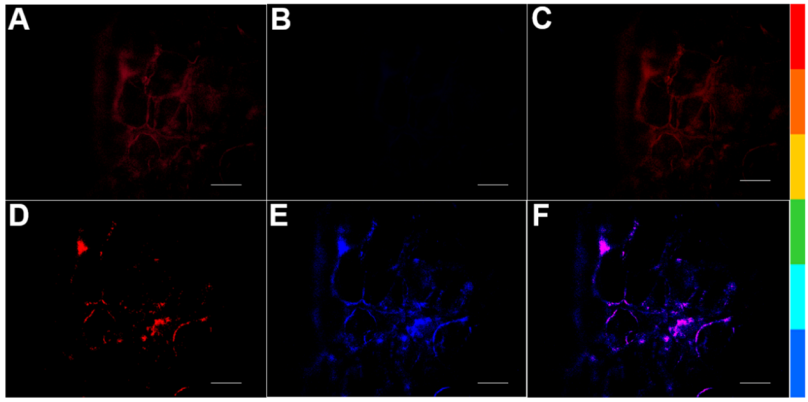

Figure 6. Fluorescence images of onion tissues incubated for 30 min without $HSO3^-$ (A−C) and with $HSO3^-$ (D−F); (A, D) red channel (580−650 nm) when excited at 453 nm; (B, E) blue channel (460−490 nm) when excited at 453 nm; (C) merged image of A−B; and (F) merged image of D−E. Scale bar: 20 μm.

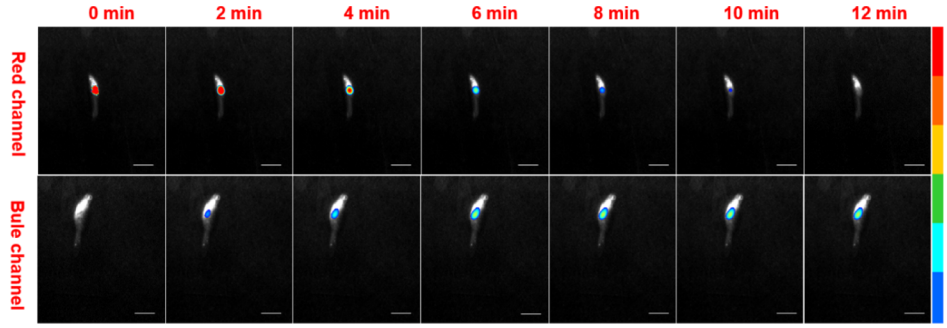

Figure 7. Fluorescence images of KQ−SO_2 with exogenous $HSO3^-$: the average fluorescence intensity ratios of the red channel and the blue channel (from 0 to 12 min). Red channel (580−650 nm) when excited at 580 nm. Blue channel (460−490 nm) when excited at 450 nm. Scale bar: 20 μm.

and KQ−SO_2 was mostly a combination reaction under these conditions. This phenomenon may be related to the combination of H^+ and $HSO3^-$, which weakens the reaction between $HSO3^-$ and KQ−SO_2. However, it is worth mentioning that the sensor still displayed a satisfactory fluorescence intensity ratio (I_{475}/I_{600}). Therefore, in this work, pH 7.4 was employed in all tests to detect $HSO3^-$.

Furthermore, in order to detect $HSO3^-$ quickly and conveniently, the paper test strip system was developed (Figure 4). Neutral filter papers when dipped in the solution of the sensor appeared orange under natural light (Figure 4A). Then, the addition of various potential interfering substances (100 μM) only $HSO3^-$ caused an obvious color change (Figure 4C). For fluorescence response, only $HSO3^-$ caused a large change from orange to blue in the fluorescence spectra of KQ−SO_2 (Figure 4B,D). The sensing behavior could be easily observed by naked eyes from the color change.

The Sensor KQ−SO_2 Detects $HSO3^-$ in Real Food Samples. Based on these above results, the sensor had a good response to $HSO3^-$ *in vitro*. In order to further verify the ability of the sensor for detecting $HSO3^-$ in food samples, the sensor was used to determine the concentration of $HSO3^-$ in real samples. As could be seen from Figure 5A,B, in these real food samples and polluted food samples, $HSO3^-$ was extracted with deionized water. After the probe KQ−SO_2 solution was added to the water samples, the fluorescent signal at I_{475}/I_{600} was recorded. The fluorescence spectra indicated that the ratio of the sensor KQ−SO_2 at I_{475}/I_{600} was significantly enhanced for polluted food samples, which was not affected by the matrix effect (Table 2). In addition, our work further confirmed the ability of KQ−SO_2 to detect $HSO3^-$ levels in the food sample and water samples (Table 2). Thus, KQ−SO_2 could quantitatively detect $HSO3^-$ in real samples.

Fluorescence Imaging of $HSO3^-$ in Onion Tissues. The potential application of KQ−SO_2 for fluorescence detection of $HSO3^-$ in onion tissues was explored. Before exploring the application of KQ−SO_2 for imaging $HSO3^-$ biological systems, the cytotoxicity of KQ−SO_2 was evaluated. The results showed that more than 85% of cells still remained alive (Figure S2), suggesting that it could be applied to biological systems. In addition, incubation of onion tissues only with KQ−SO_2 (5.0 μM) for 30 min at 37 °C was performed and then fluorescence images were taken. It was obvious that the fluorescence did not appear in the blue channel (460−490 nm) but in the red channel (580−650 nm) by the one-photon confocal laser microscope (OPM) (Figure 6A,B). After, being further incubated upon addition of $HSO3^-$ (20 μM) for 30 min, fluorescent signals decreased significantly in the red channel and increased in the blue channel (Figure 6D,E). These data suggested that the probe KQ−SO_2 was tissue penetrable and suitable for detecting the changes of $HSO3^-$ in onion tissues.

Fluorescence Imaging of $HSO3^-$ in the Zebrafish Model. Inspired by the excellent property of the sensor in onion tissue detection, finally, the newly designed sensor KQ−SO_2 was further utilized to detect $HSO3^-$ in a zebrafish model. The detection of the zebrafish model was determined by a BiospaceLab PhotonIMAGER, as shown in Figure 7. Then, the

https://doi.org/10.1021/acs.jafc.1c00592
J. Agric. Food Chem. 2021, 69, 4894−4902

zebrafish was injected with KQ−SO_2 and $HSO3^-$ in the belly for real-time imaging; bright fluorescence in the blue channel and weak fluorescence in the red channel were observed within 0−12 min. These time-dependent red fluorescence reduction and blue fluorescence enhancement were attributed to the consumption of $HSO3^-$ for the Michael addition reaction, inducing sensor's π-conjugation to be blocked. Therefore, these results further confirmed that KQ−SO_2 not only had the ability to detect in an animal model but also was capable of dynamic detection of $HSO3^-$ in zebrafish in real time.

In summary, we have demonstrated that an ICT fluorescent probe, KQ−SO_2, could be constructed from carbazole and positively charged indoline for the ratiometric detection of $HSO3^-$. Importantly, the sensor displayed high selectivity, fast response, and great sensitivity, which benefited from the advantageous photophysical properties that resulted from the reaction between $HSO3^-$ and KQ−SO_2. Specifically, non-overlapping bright emission bands are observed due to a large distance (225 nm) between the dual-emission peaks for the fluorescence imaging. Moreover, KQ−SO_2 could rapidly detect $HSO3^-$ in real food samples, onion tissues, and zebrafish. The novel reaction-based fluorescent sensor is promising to be used as an efficient tool in physiology and pathology.

■ ASSOCIATED CONTENT

Supporting Information

The Supporting Information is available free of charge at https://pubs.acs.org/doi/10.1021/acs.jafc.1c00592.

Comparison of various methods, parameters, probes, and their structures reported in literature with our probe in real food detection; MS spectra of the reaction of probe with sodium bisulfite in PBS; viability of HeLa cells at various concentrations; time-dependent fluorescence intensity ratios of the probe upon the addition of sodium bisulfite; and NMR spectra (PDF)

■ AUTHOR INFORMATION

Corresponding Author

Liyi Zhou − *National Engineering Laboratory for Deep Process of Rice and Byproducts, College of Food Science and Engineering, Central South University of Forestry and Technology, Changsha 410004, Hunan, China;* orcid.org/0000-0001-7181-9353; Email: zhouly0817@163.com

Authors

Gangqiang Yuan − *National Engineering Laboratory for Deep Process of Rice and Byproducts, College of Food Science and Engineering, Central South University of Forestry and Technology, Changsha 410004, Hunan, China*

Qiaomei Yang − *National Engineering Laboratory for Deep Process of Rice and Byproducts, College of Food Science and Engineering, Central South University of Forestry and Technology, Changsha 410004, Hunan, China*

Haiyuan Ding − *National Engineering Laboratory for Deep Process of Rice and Byproducts, College of Food Science and Engineering, Central South University of Forestry and Technology, Changsha 410004, Hunan, China*

Libin Tan − *National Engineering Laboratory for Deep Process of Rice and Byproducts, College of Food Science and Engineering, Central South University of Forestry and Technology, Changsha 410004, Hunan, China*

Longpeng Peng − *National Engineering Laboratory for Deep Process of Rice and Byproducts, College of Food Science and Engineering, Central South University of Forestry and Technology, Changsha 410004, Hunan, China*

Complete contact information is available at: https://pubs.acs.org/10.1021/acs.jafc.1c00592

Notes

The authors declare no competing financial interest.

■ ACKNOWLEDGMENTS

This work was supported by the Natural Science Foundation of China (NSFC, grants 21605046), the Hunan Provincial Natural Science Foundation of China (no. 2017JJ3060), and the Changsha Science and Technology Bureau Fund Project (no. kq1901140).

■ REFERENCES

(1) Wedzicha, B. L. *Chemistry of Sulphur Dioxide in Foods*; Elsevier Applied Science Publishers: London and New York, 1984; pp 275−311.

(2) Yang, X.-F.; Guo, X.-Q.; Zhao, Y.-B. Novel spectrofluorimetric method for the determination of sulfite with rhodamine b hydrazide in a micellar medium. *Anal. Chim. Acta* **2002**, *456*, 121−128.

(3) Fazio, T.; Warner, C. R. A review of sulphites in foods: analytical methodology and reported findings. *Food Addit. Contam.* **1990**, *7*, 433−454.

(4) Sang, N.; Yun, Y.; Li, H.; Hou, L.; Han, M.; Li, G. SO_2 inhalation contributes to the development and progression of ischemic stroke in the brain. *Toxicol. Sci.* **2010**, *114*, 226−236.

(5) Sang, N.; Yun, Y.; Yao, G.-y.; Li, H.-y.; Guo, L.; Li, G.-k. SO_2-induced neurotoxicity is mediated by cyclooxygenases-2-derived prostaglandin E2 and its downstream signaling pathway in rat hippocampal neurons. *Toxicol. Sci.* **2011**, *124*, 400−413.

(6) Lee, W. J.; Teschke, K.; Kauppinen, T.; Andersen, A.; Jäppinen, P.; Szadkowska-Stanczyk, I. Mortality from lung cancer in workers exposed to sulfur dioxide in the pulp and paper industry. *Environ. Health Perspect.* **2020**, *110*, 991−995.

(7) Finkel, T.; Holbrook, N. J. Oxidants, oxidative stress and the biology of ageing. *Nature* **2000**, *408*, 239−247.

(8) *Sulfites in Standardized Food*; Code of Federal Regulations, Part 130, Title 21, 2018.

(9) WHO *Food Additives Series NO. 5*; World Health Organization: Geneva, 1974.

(10) General Administration of Quality Supervision *Inspection and Quarantine of the People's Republic of China*; 2014, GB2760-2014.

(11) Sun, J.; Bai, Y.; Ma, Q.; Zhang, H.; Wu, M.; Wang, C.; Tian, M. A FRET-based ratiometric fluorescent probe for highly selective detection of hydrogen polysulfides based on a coumarin-rhodol derivative. *Spectrochim. Acta, Part A* **2020**, *241*, 118650.

(12) Ma, Q.; Wang, C.; Mao, G.; Tian, M.; Sun, J.; Feng, S. An endoplasmic reticulum-targeting and ratiometric fluorescent probe for hypochlorous acid in living cells based on a 1,8-naphthalimide derivative. *New J. Chem.* **2020**, *44*, 18389−18398.

(13) Bai, Y.; Wu, M.-X.; Ma, Q.-J.; Wang, C.-Y.; Sun, J.-G.; Tian, M.-J.; Li, J.-S. A FRET-based ratiometric fluorescent probe for highly selective detection of cysteine based on a coumarin-rhodol derivative. *New J. Chem.* **2019**, *43*, 14763−14771.

(14) Zhang, T.; Yin, C.; Zhang, Y.; Chao, J.; Wen, G.; Huo, F. Mitochondria-targeted reversible ratiometric fluorescent probe for monitoring SO2/HCHO in living cells. *Spectrochim. Acta, Part A* **2020**, *234*, 118253.

(15) Huang, Y.; Zhang, Y.; Huo, F.; Yin, C. FRET-dependent single/two-channel switch endowing a dual detection for sulfite and its organelle targeting applications. *Dyes Pigm.* **2021**, *184*, 108869.

(16) Feng, H.; Liu, J.; Qaitoon, A.; Meng, Q.; Sultanbawa, Y.; Zhang, Z.; Xu, Z. P.; Zhang, R. Responsive small-molecule

luminescence probes for sulfite/bisulfite detection in food samples. *TrAC, Trends Anal. Chem.* **2021**, *136*, 116199.
(17) O'Neil, E. J.; Smith, B. D. Anion recognition using dimetallic coordination complexes. *Coord. Chem. Rev.* **2006**, *250*, 3068−3080.
(18) Zheng, X.-L.; Li, H.; Feng, W.; Xia, H.-C.; Song, Q.-H. Two-step sensing, colorimetric and ratiometric fluorescent probe for rapid detection of bisulfite in aqueous solutions and in living cells. *ACS Omega* **2018**, *3*, 11831−11837.
(19) Sun, Y.; Zhao, D.; Fan, S.; Duan, L.; Li, R. Ratiometric fluorescent probe for rapid detection of bisulfite through 1,4-addition reaction in aqueous solution. *J. Agric. Food Chem.* **2014**, *62*, 3405−3409.
(20) Liu, Y.; Li, K.; Wu, M.-Y.; Liu, Y.-H.; Xie, Y.-M.; Yu, X.-Q. A mitochondria-targeted colorimetric and ratiometric fluorescent probe for biological SO_2 derivatives in living cells. *Chem. Commun.* **2015**, *51*, 10236−10239.
(21) Zhang, Q.; Zhang, Y.; Ding, S.; Zhang, H.; Feng, G. A nearinfrared fluorescent probe for rapid, colorimetric and ratiometric detection of bisulfite in food, serum, and living cells. *Sens. Actuators, B* **2015**, *211*, 377−384.
(22) Zhou, F.; Sultanbawa, Y.; Feng, H.; Wang, Y.-L.; Meng, Q.; Wang, Y.; Zhang, Z.; Zhang, R. A new red-Emitting fluorescence probe for rapid and effective visualization of bisulfite in food samples and live animals. *J. Agric. Food Chem.* **2019**, *67*, 4375−4383.
(23) Ma, Y.; Tang, Y.; Zhao, Y.; Lin, W. Rational design of a reversible fluorescent probe for sensing sulfur dioxide/formaldehyde in living cells, zebrafish, and living mice. *Anal. Chem.* **2019**, *91*, 10723−10730.
(24) Ito, S.; Muguruma, N.; Kakehashi, Y.; Hayashi, S.; Okamura, S.; Shibata, H.; Okahisa, T.; Kanamori, M.; Shibamura, S.; Takesako, K.; Nozawa, M.; Ishida, K.; Shiga, M. Development of fluorescenceemitting antibody labeling substance by near-infrared ray excitation. *Bioorg. Med. Chem. Lett.* **1995**, *5*, 2689−2694.

https://doi.org/10.1021/acs.jafc.1c00592
J. Agric. Food Chem. 2021, 69, 4894−4902